Influence of a Large-Eddy-Breakup-Device on the Turbulent Interface of Boundary Layers

C. Chin[1], N. Hutchins[1], A. Ooi[1], R. Örlü[2], P. Schlatter [2] and J. P. Monty[1]
[1]*Dept of Mechanical Engineering, University of Melbourne, Victoria 3010, Australia*
[2]*Linné FLOW Centre, KTH Mechanics, SE-100 44 Stockholm, Sweden*

chincc@unimelb.edu.au

Abstract

This paper investigates the effects of implementing a large-eddy break-up device (LEBU) on the growth of the boundary layer. The LEBU is placed at a wall-normal distance of 0.8δ (local boundary layer thickness) from the wall. A detail analysis of the interaction between the LEBU and the turbulent/non-turbulent interface (TNTI) is performed and the LEBU is found to to delay the growth of the turbulent boundary layer. At the near-wall, the LEBU acts to reduce global skin friction drag. It is found that the structures along the TNTI is different between that of the LEBU and a normal developing turbulent boundary layer, where the structures appear smaller in length and width in the LEBU case. In addition, the LEBU disrupts the entrainment of the freestream high momentum flow into the boundary layer.

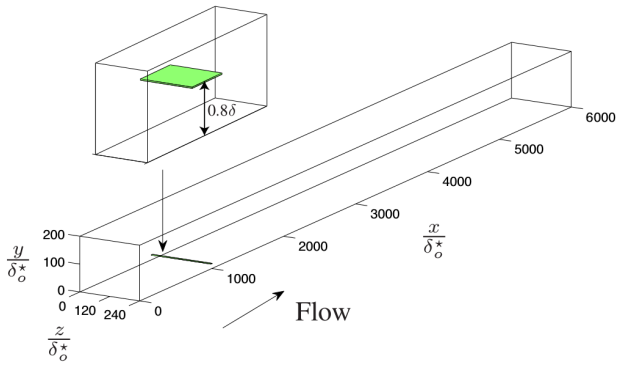

Figure 1: Computational domain of the turbulent boundary layer LES. The LEBU is imposed after a complete washthrough and performed as a separate simulation

1 Introduction

Coherent structures have been found to play a major role in the growth and evolution of turbulent boundary layers (TBLs) Townsend(1956), thereby opening doors for the beneficial manipulation and control Corke(1981). These lead to the birth of large-eddy break-up devices (LEBUs), which consist of one or more thin plates or airfoils placed parallel to the wall emerged in the outer part of turbulent boundary layers, and act to 'break up' the 'large-eddies'. These devices were found to be capable of reducing the local skin friction by tens of percentage, however, no clear physical explanation of the mechanism has been presented. With the renewed interest in the very large-scale motions (VLSMs) as reported by Hutchins and Marusic (2007) and their influence that extends to the wall (Mathis et al 2009), re-examination of LEBUs (and other OLDs) seems pertinent, especially given recent advances in our ability to simulate developing turbulent boundary layers. One area of interest is in the turbulent/non-turbulent interface (TNTI), where it is defined as a line or surface that separates the turbulent region from the non-turbulent region. The TNTI is an important parameter in the study of boundary layers as it characterises the growth of the boundary layer and the entrainment process of high momentum flow from the free stream into the turbulent region of the boundary layer. Since the primary purpose of the LEBU is to break up large eddies, this work investigates the influence of the LEBU on the largest-scales located at the turbulent/non-turbulent interface (TNTI).

2 Methodology

The TBL and LEBU numerical datasets are taken from Chin et al (2015). The dataset is a well-resolved large eddy simulation (LES) of a large-eddy break-up (LEBU) device in a spatially evolving turbulent boundary layer up to $Re_\theta \approx 4300$ is performed. Here the streamwise, wall-normal and spanwise directions are denoted as x, y and z with corresponding velocities represented as $U+u$, $V+v$ and $W+w$. The inlet boundary condition is set to be a laminar Blasius boundary layer profile with $Re_{\delta^\star_o} = 450$, where $\delta^\star_o$ is the displacement thickness at the inlet of the computational domain. A low amplitude forcing is imposed close to the inlet to *trip* the flow in order to achieve turbulent transition earlier. The LEBU is a flat plate that is implemented via an immersed boundary method as shown in figure 1. The LEBU is placed at a wall-normal location of 0.8δ, where δ is the local boundary layer thickness and at a streamwise location of $x/\delta \approx 45$ downstream from the inlet. The computational domain is $L_x \times L_y \times L_z = 6000\delta^\star_o \times 200\delta^\star_o \times 240\delta^\star_o$ in the streamwise, wall-normal and spanwise directions respectively (or $L_x/\delta \times L_y/\delta \times L_z/\delta \approx 272 \times 9 \times 11$). The associated number of spectral collocated points is 6144 $\times$ 513 $\times$ 512.

3 Results

It was previously reported by Chin et al (2015) that the maximum skin friction (c_f) reduction for the LEBU is approximate 12% at $x/\delta \approx 25$ downstream of the LEBU shown in figure 2. The red line denotes the TBL and the blue line is for the LEBU c_f profiles. There are

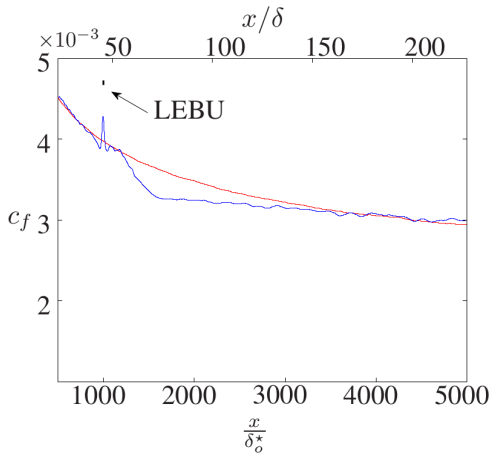

Figure 2: Comparison of the (a) skin friction coefficient c_f and (b) Reynolds number Re_θ based on free-stream velocity and momentum thickness between LEBU and TBL. Red line denotes TBL and the blue line is LEBU

three regions of interest to investigate for the LEBU case, namely (*i*) x/δ around the vicinity of the LEBU; (*ii*) $x/\delta \approx 25$, which is the location of maximum c_f reduction and (*iii*) $x/\delta \approx 160$, where the c_f appears to collapse back to the TBL profile. Since the LEBU is located at close to the edge of the boundary layer, the effects of the interaction of the LEBU and the boundary layer are further investigated.

The TNTI is detected using the instantaneous height of the boundary layer at $U = 0.99U_\infty$. The TNTI obtained using this method has been compared to the detection method using kinetic energy by Chauhan et al (2014) and found to be similar. Hence we adopted the identification of the TNTI to be $U = 0.99U_\infty$. Figure 3 shows an illustration of the method employed. The white contour denotes the instantaneous height H (the fluctuation is defined as h) of the TNTI at various streamwise location for a given timestep and the black line indicates the mean boundary layer thickness. Figure refTNTI compares the fluctuation of the TNTI height h normalised by the local boundary layer thickness δ_L of the TBL (top figure) and the LEBU (bottom figure). In the TBL case, the h/δ_L profile exhibits consistent fluctuation values across the entire x/δ. It is observed that these fluctuations steadily increase in size (length and width) as x/δ increases. This increase in size is consistent with increasing Reynolds number as the boundary layer develops from left to right. In the LEBU case, the black solid line denoted the streamwise location of the LEBU, prior to the LEBU, the h/δ_L profile is similar to the TBL. However, immediately behind the LEBU, the fluctuation is severely attenuated. This effect persists for a streamwise distance of $x/\delta \approx 25$ downstream of the LEBU (indicated by the black dash-line in the LEBU case). Subsequently, the h/δ_L profile appears to revert back to that of the TBL, one might notice the length-scales of these h/δ_L fluctuations are slightly weaker and shorter than that of the TBL.

Figure 5 displays the rms profile of h for both TBL and LEBU as a function of streamwise distance. Here it is immediately clear that after the LEBU, there is severe attenuation of the fluctuation intensity h. The effect of this attenuation persists for a streamwise distance $x/\delta \approx 100$ downstream of the LEBU before collapsing back to the TBL profile. It is interesting to note that this distance of $x/\delta \approx 100$ corresponds to the distance we notice

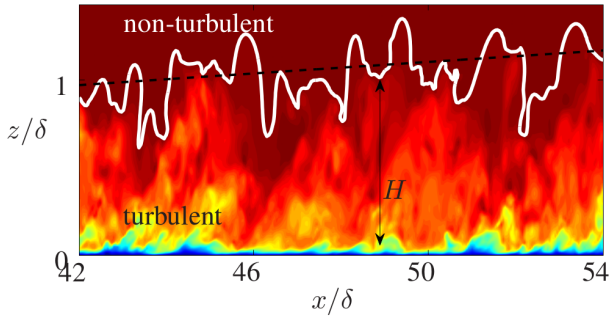

Figure 3: Detection method for the turbulent/non-turbulent interface. The interface wall-normal height (H) is defined as $0.99U_\infty$. The white contour is at $U = 0.99U_\infty$, black contour is the mean boundary layer thickness

drag reduction in the c_f (see figure 2). The results suggest that apparently the generation of vortices from the trailing edge of the LEBU does not add to the fluctuation of the TNTI. The LEBU seems to creates a shear layer (due to the wake) that stabilises the TNTI by preventing entrainment of the non-turbulent region containing large amount of energy and momentum into the turbulent boundary layer. This might be the mechanism that causes skin friction drag reduction seen in figure 2.

Next, the two point correlation will be utilised to investigate the difference in structure size in the TNTI. Two point correlation have been used to understand average structure characteristics and help identify coherent structures (see Brown and Thomas 1977). the correlation equation is given in (1).

$$R_{IJ} = \frac{\overline{I(x,y,z)J(x+\Delta x, y+\Delta y, z+\Delta z)}}{\sigma_I \sigma_J}, \quad (1)$$

where I and J correspond to the signals of interest. If $I = J$ it is a two-point correlation, and when $I \neq J$ it is a cross correlation. Here σ refers to the standard deviation, and Δx, Δy and Δz are the spatial distances in the streamwise and wall-normal and spanwise directions respectively. The overbar denotes the spatial and temporal average. Figure 6 presents the cross correlation contours of h for TBL and LEBU at various locations $x/\delta \approx 25$, 100 and 160 downstream of the LEBU. The left column presents the results for the LEBU and the right column is for the TBL. Note that the x and y axes are normalised by the local boundary layer thickness at its corresponding streamwise location.

Figure 6(a,b) is at $x/\delta \approx 25$, which is where the maximum c_f reduction occurs. It is clear that the average structure at the TNTI for the LEBU is narrower and shorter. This is most likely due to the wake of the LEBU that is interacting with the boundary layer. Further downstream at $x/\delta \approx 100$ (figure 6 c,d), it appears that the structures are similar between TBL and LEBU. However, upon closer inspection near the peak correlation contours, the LEBU is slightly narrower in width as compared to the TBL. At distance $x/\delta \approx 160$ downstream of the LEBU, where the c_f profile of the LEBU collapses back to the TBL, the structures remain different. The structure in the TBL still is longer and wider when compared to the LEBU. Across the different streamwise locations, there is evidence to suggest that the LEBU acts to permanently alter the TNTI.

To further investigate the effects of the LEBU on the

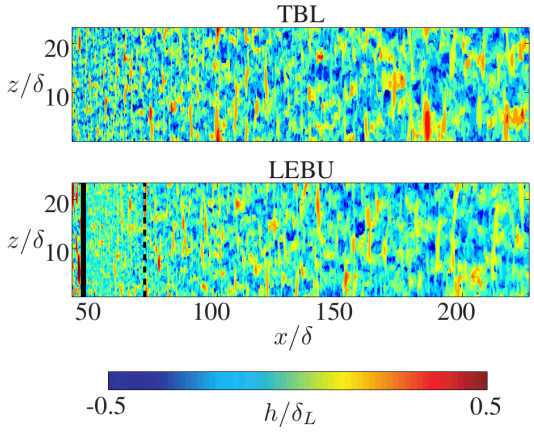

Figure 4: Contour plots of the TNTI fluctuating height h for TBL (top) and LEBU (bottom). The black solid line denotes the streamwise location of the LEBU. The black dash-line is at $x/\delta \approx 25$ downstream of the LEBU

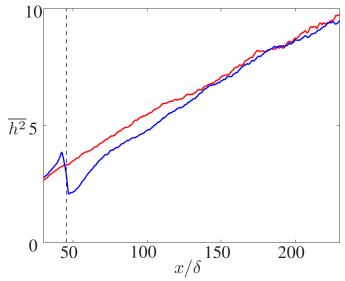

Figure 5: Comparison of the rms of h between TBL and LEBU. The red line denotes TBL and the blue line is LEBU. The black dash-line denotes the location of the LEBU

entrainment process, correlation between h and u is computed for various wall-normal distances of u. This allows the study of the direct relationship and influence of the TNTI on the velocity at a given wall-normal height. Here we have chosen the wall-normal locations of $y/\delta_L \approx 0.1$, 0.5 and 0.8, represented by red, blue and black lines respectively in figure 7. Figure 7(a) shows the results for the TBL and (b) for the LEBU, the LEBU location is denoted by the solid grey line. The results from the TBL show that there is consistently strong influence (constant correlation coefficient, $R_{hu} \approx 0.4$) of the TNTI on the velocity profile at wall-normal location of $y/\delta_L \approx 0.8$ as the boundary layer develops. The influence of the TNTI on the velocity field at $y/\delta_L \approx 0.5$ appears relatively weak with $R_{hu} \approx 0.1$, which displays a somewhat linear increase in R_{hu} with x/δ. This is expected as the fluctuation of the TNTI will increase in strength as Reynolds number increases with x/δ. Within the logarithmic region $y/\delta_L \approx 0.1$, there seems to be negligible influence of the TNTI on the velocity field. In the LEBU case presented in figure 7(b), a similar trend to the TBL is noticed for R_{hu} at wall-normal distance of $y/\delta_L \approx 0.1$. The result for $y/\delta_L \approx 0.5$ appears similar to that of the TBL except at the streamwise location where the LEBU is located. At this location, there is a sudden mild spike in the correlation coefficient (blue line). As the TNTI fluctuates in the wall-normal direction. This is probably due to the presence of the LEBU that increases the intermittency at $y/\delta_L \approx 0.5$ leading to the increase in R_{hu}. The most interesting result is at $y/\delta_L \approx 0.8$. The correlation R_{hu} is similar to that of the TBL preceding the LEBU, however, at the LEBU, there is sudden decrease in correlation. This can again be explained by the wall-normal location of the LEBU (at $y/\delta_L \approx 0.8$), which has essentially zero velocity. Immediately after the LEBU, the TNTI clearly does not correlate with the shedding of vortices at the trailing edge of the LEBU, hence the low R_{hu}. The wake seems to dissipate relatively quickly and the R_{hu} collapses back to match the TBL profile at $x/\delta \approx 100$. This agrees with the earlier discussion that the wake disrupts the entrainment process. This is further evidence that the entrainment process is critical to understanding the drag reduction seen in c_f.

4 Conclusions

A detail investigation on the effects of the LEBU on the turbulent boundary layer is performed using high fidelity numerical simulation dataset. The results are compared to a spatially evolving turbulent boundary layer. The LEBU acts to permanently change the characteristics of the TNTI resulting in a shorter and narrower dominant structure at the interface and attenuates the fluctuation intensity of the TNTI. Further correlation results show that the LEBU clearly disrupts the entrainment of the high momentum flow in the freestream into the turbulent boundary layer. There is evidence to support that the mechanism for skin friction drag reduction is due to the disruption of the entrainment process. Future work will be focused on the near-wall statistics to investigate how the turbulent structures are alter in the presence of the LEBU.

Acknowledgments

This research was undertaken with the assistance of resources provided at the NCI NF through the National Computational Merit Allocation Scheme supported by the Australian Government. Computer time was also provided by SNIC (Swedish National Infrastructure for Computing). The simulations were run at the Centre for Parallel Computers (PDC) at the Royal Institute of Technology (KTH). The authors also acknowledge the financial support of the Australian Research Council.

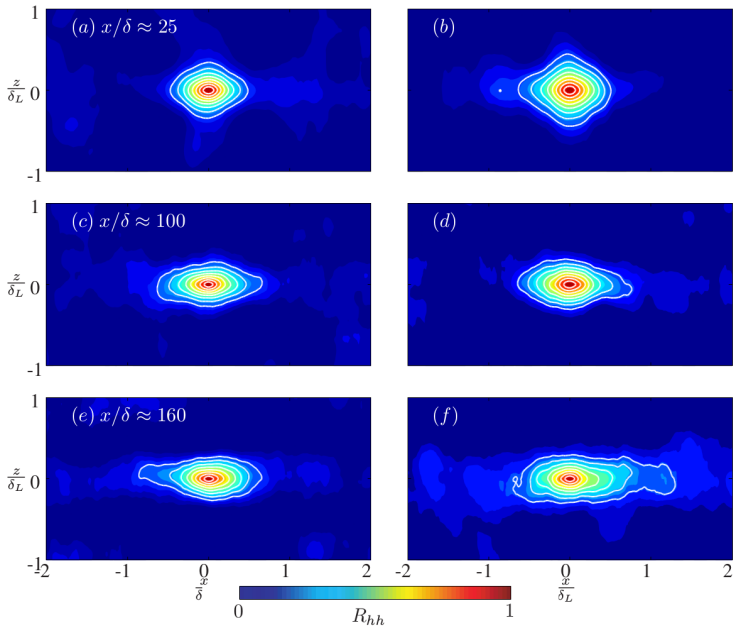

Figure 6: Cross correlation (R_{hh}) contour map of the TNTI fluctuation height (h) at a streamwise location of $x/\delta \approx 25$ (a,b); $x/\delta \approx 100$ (c,d) and $x/\delta \approx 160$ (e,f) downstream of the LEBU. Left: TBL; Right: LEBU. The x-y axes are normalised by the local boundary layer thickness δ_L ($\approx 30\delta_o^\star$, $53\delta_o^\star$ & $69\delta_o^\star$ respectively). Contour levels begin at R_{hh} = 0.1 with increments of 0.1

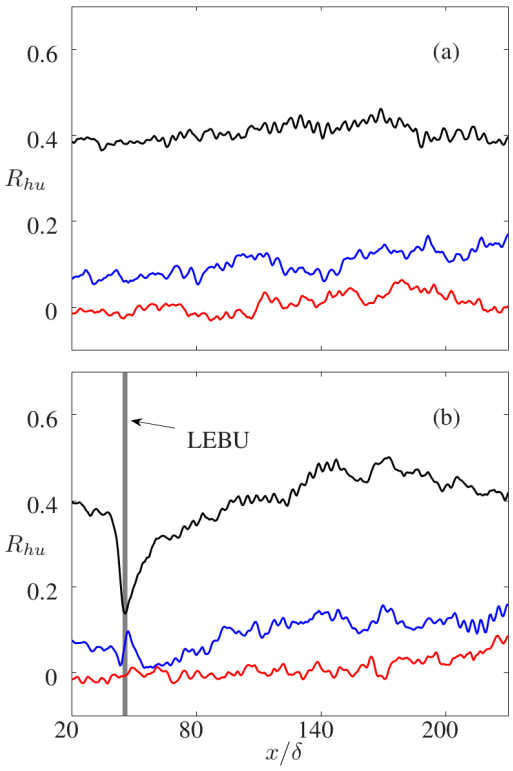

Figure 7: Cross correlation (R_{hu}) of h and u for (a) TBL and (b) LEBU. Red line denotes correlation of h with u at $y/\delta_L \approx 0.1$; blue line is for correlation of h with u at $y/\delta_L \approx 0.5$ and black line is for correlation of h with u at $y/\delta_L \approx 0.8$. The grey solid line denotes the streamwise location of the LEBU

References

Townsend, A. A. (1976) The structure of turbulent shear flow. Cambridge University Press, 2nd ed.

Corke, T. C., Guezennec, Y. and Nagib, H.M. (1981) Modification in drag of turbulent boundary layers resulting from manipulation of large-scale structures. NASA CR 3444.

Hutchins, N. and Marusic, I. (2007) Evidence of very long meandering features in the logarithmic region of turbulent boundary layers. J. Fluid Mech. 579, 1-28.

Mathis, R., Hutchins, N. and Marusic, I. (2009) Large-scale amplitude modulation of the small-scale structures in turbulent boundary layers. J. Fluid Mech. 628, 311-337.

Chin, C., Monty. J., Hutchins, N. Ooi, A., Örlü, R. and Schlatter, P. (2015) Simulation of a large-eddy-break-up device (LEBU) in a moderate Reynolds number turbulent boundary layer, TSFP 9, Paper 1A-3.

Chauhan, K., Philip, J. and Marusic, I. (2014) Scaling of the turbulent/non-turbulent interface in boundary layers. J. Fluid Mech. 751, 298–328.

Brown, G. L. and Thomas, A. S. W. (1977) Large structure in a turbulent boundary layer. Physics of Fluids 20,10, S243 - S252.